From Powder to Solution: Hydration Dependence of Human Hemoglobin Dynamics Correlated to Body Temperature

A. M. Stadler,[†‡] I. Digel,[§] J. P. Embs,[¶‖] T. Unruh,[††] M. Tehei,[‡‡§§] G. Zaccai,[†*] G. Büldt,[‡] and G. M. Artmann[§]
[†]Institut Laue-Langevin, 38042 Grenoble, France; [‡]Research Centre Jülich, 52425 Jülich, Germany; [§]Institute of Bioengineering, Aachen University of Applied Science, 52428 Jülich, Germany; [¶]Laboratory for Neutron Scattering ETH Zurich and Paul Scherrer Institut, 5232 Villigen PSI, Switzerland; [‖]Saarland University, Physical Chemistry, 66123 Saarbrücken, Germany; [††]Technische Universität München, Forschungsneutronenquelle Heinz Maier-Leibnitz (FRM II), 85747 Garching, Germany; [‡‡]School of Chemistry, University of Wollongong, 2522 Wollongong, Australia; and [§§]Australian Institute of Nuclear Science and Engineering (AINSE), Menai, Australia

ABSTRACT A transition in hemoglobin (Hb), involving partial unfolding and aggregation, has been shown previously by various biophysical methods. The correlation between the transition temperature and body temperature for Hb from different species, suggested that it might be significant for biological function. To focus on such biologically relevant human Hb dynamics, we studied the protein internal picosecond motions as a response to hydration, by elastic and quasielastic neutron scattering. Rates of fast diffusive motions were found to be significantly enhanced with increasing hydration from fully hydrated powder to concentrated Hb solution. In concentrated protein solution, the data showed that amino acid side chains can explore larger volumes above body temperature than expected from normal temperature dependence. The body temperature transition in protein dynamics was absent in fully hydrated powder, indicating that picosecond protein dynamics responsible for the transition is activated only at a sufficient level of hydration. A collateral result from the study is that fully hydrated protein powder samples do not accurately describe all aspects of protein picosecond dynamics that might be necessary for biological function.

INTRODUCTION

Hemoglobin (Hb) in red blood cells and at high concentration in solution shows a variety of interesting effects (1). Micropipette experiments with aspirated single human red blood cells found a sudden passage phenomenon of the cells at a transition temperature $T_{\text{Pipette}} = 36.4 \pm 0.4^{\circ}\text{C}$ close to human body temperature (36.6°C or 309.8 K) (2). The diameter of the micropipette (~1.5 μm) was small compared to the entire cells (~7 μm). Part of the cellular membrane is aspirated into the tight pipette tip and forms a tongue. The major fraction of the cell forms a sphere filled with Hb outside of the pipette. At temperatures lower than body temperature the cell cannot pass into the pipette completely and blocks the tip. Above body temperature, the trailing sphere can be compressed easily and all cells pass into the pipette with no apparent resistance (2). Under normal conditions the concentration of Hb in red blood cells is ~330 mg/mL (3). During the aspiration process below body temperature intracellular water is pressed out of the red blood cell, and it was estimated that Hb concentration reaches values of more than ~500 mg/mL (2). Viscosity measurements were carried out on Hb solutions between 330 mg/mL and 500 mg/mL to study the flow properties at such concentrations (2). The experiments found a sharp drop in viscosity in Arrhenius plots at concentrations higher than 450 mg/mL at body temperature. The drop was absent at the physiological concentration of 330 mg/mL. The results were interpreted as a colloidal phase transition in highly concentrated Hb solution from a gel-like to a fluid state at body temperature (2,4).

It has been further investigated, if the transition temperature of Hb is correlated to changes of the protein structure; the thermal stability of Hb secondary structure was investigated with circular dichroism spectroscopy (CD) (5). The study showed a pronounced loss of α-helical content at $T_{\text{CD}} = 37.2 \pm 0.6^{\circ}\text{C}$, which is again close to human body temperature. Interestingly, further CD experiments established that thermal stability of Hb secondary structure of different animals is directly correlated to the corresponding body temperature of the species. The results ranged from $T_{\text{CD}} = 34.0 \pm 0.5^{\circ}\text{C}$ for the duck-billed platypus (body temperature $33.0 \pm 1.0^{\circ}\text{C}$) to $T_{\text{CD}} = 42.0 \pm 1.0^{\circ}\text{C}$ for a bird, the spotted nutcracker (body temperature $42.2 \pm 0.5^{\circ}\text{C}$) (6,7). It has been speculated that the mechanism behind Hb temperature behavior might be partial unfolding of the α-helical structure at body temperature, which goes in hand with an increase in surface hydrophobicity that promotes protein aggregation (6).

Energy resolved incoherent neutron scattering is a powerful technique for the study of dynamics of biological macromolecules and its dependence on environmental conditions. Protein dynamics has been studied with neutron scattering in hydrated powders (8,9) and as a response to environmental conditions, in particular to the level of hydration (10–12). In the past years, neutron scattering has been applied to study protein dynamics in whole cells in vivo (13–16) and in solution (17–19). Incoherent neutron scattering is dominated by hydrogen atom motions as their incoherent scattering cross section is one order of magnitude bigger than that of all other

Submitted January 12, 2009, and accepted for publication March 30, 2009.

*Correspondence: zaccai@ill.fr

Editor: Marcia Newcomer.

0006-3495/09/06/5073/9 $2.00

doi: 10.1016/j.bpj.2009.03.043

elements that usually occur in biological matter, and deuterium (20). The technique probes average protein dynamics because hydrogen atoms are uniformly distributed in the natural abundance protein. The time and length scales of molecular motions that are accessible are determined by the energy resolution and the scattering vector range of the instrument, respectively. In general, the method covers the picosecond to nanosecond time range and angstrom length scale. At this time-length scale, hydrogen atoms that are covalently bound to amino acid side chains reflect the dynamical behavior of these bigger chemical units (21–23). Below a so-called dynamical transition temperature of ~180–240 K protein dynamics is predominantly harmonic. Harmonic motions correspond to vibrations of atoms around their structural equilibrium positions. Above the dynamical transition, and at sufficient hydration, additional anharmonic motions are activated (8,9,24). Depending on the energy resolution and scattering vector range of the neutron spectrometer, a second inflection in the thermal displacements, which is hydration-independent, was observed at a temperature between 100 and 150 K, and has been attributed to methyl group rotations (10,25–27). These local jumps contribute to the sampling of a large number of conformational substates that are responsible for the entropic stabilization of proteins (28). From elastic incoherent neutron scattering (EINS) mean-square displacements $\langle u^2 \rangle$ of the thermal cloud of atomic motions can be determined. The measured $\langle u^2 \rangle$ include both vibrational and diffusive motions (21). Quasielastic neutron scattering (QENS) on the other hand, enables us to distinguish between vibrational and diffusive components (29). The technique allows the quantification of internal diffusion coefficients, residence times and the determination of the average geometry of motions.

Protein dynamics has been interpreted with a model of a quasi-harmonic average potential well for the complex macromolecular force field (30,31). In this sense, protein flexibility was defined as the amplitude of atomic motions $\sqrt{\langle u^2 \rangle}$ that corresponds to the width of the potential well. Protein thermal stability would correspond to the depth of the well (32,33). A mean effective force constant $\langle k' \rangle$ can be obtained from the dependence of the $\langle u^2 \rangle$ as function of temperature. This mean effective force constant, called resilience, describes the shape of the well (31). Many conformational substates exist within the average well and are sampled by localized jump-diffusion (28). The geometry and activation energy of localized jumps can be determined by QENS.

Recently, we measured protein dynamics of Hb in human red blood cells in vivo with QENS (15). At temperatures higher than human body temperature, amino acid side chains dynamics showed a change in the geometry of motion toward larger volumes than expected from normal temperature dependence. This change under physiological hydration conditions was interpreted as a result of partial unfolding of Hb at body temperature. The partially unfolded state above body temperature was found to be less resilient than Hb below body temperature. Our goal in this study was to investigate in detail with neutron scattering from powder to solution, how the different motions of human Hb depend on hydration. A change in the geometry of amino acid side chain dynamics was identified close to human body temperature in concentrated Hb solution. Fully hydrated Hb powder showed the well known dynamical transition at ~180–240 K, but the change in the geometry of protein motions at body temperature was not found.

MATERIAL AND METHODS

Sample preparation

Human Hb was purchased from Sigma (St. Louis, MO). To remove the exchangeable hydrogen atoms, ~1 g protein was dissolved in 10 mL D_2O and lyophilized afterward. For the preparation of the hydrated powder sample, D_2O exchanged Hb powder was dried over silica gel until no further loss of weight was observed. The dried powder was then rehydrated in D_2O atmosphere to a level of 0.4 g D_2O/1 g protein. That level is not sufficient to cover the protein surface with a complete monolayer (34), but this amount of nonfreezing water permits the onset of anharmonic motions above the dynamical transition temperature of ~180–240 K (35). In this study, we consider this as one full hydration layer. For the preparation of the Hb solution sample, D_2O buffer (0.1 M KCl, 61.3 mM K_2HPO_4, 5.33 mM KH_2PO_4, pD 7.4) was added to the D_2O exchanged protein powder to a level of 1.1 g D_2O/1 g. The obtained concentration (570 mg/mL) corresponds to ~3 hydration layers. The concentration of potassium buffer was chosen to resemble saline conditions in whole cells (36), but it shall be noted that the choice of saline buffer can have an influence on protein dynamics (37). The samples were rapidly sealed in flat aluminum sample holders for the experiments. It was checked by weighting that there occurred no loss of sample material during the experiment. The incoherent scattering cross section of Hb in the concentrated solution was estimated to be >96% and in hydrated powder to be >98%. Therefore, we neglected the contribution of the D_2O solvent to the measured data. Hemoglobin from lyophilized powder was predominantly in the met state (~90%) as determined with ultraviolet/visible spectroscopy. As shown by Perutz et al. the tertiary and quaternary structure of methemoglobin is very similar to that of oxyhemoglobin (38). All used buffers were degassed before usage and did not contain any reducing agents. Therefore Hb is supposed to be in the met state throughout the experiments.

Neutron scattering experiments

The experiments were carried out on the cold neutron multi-disk-chopper time-of-flight spectrometer TOFTOF (39) at the research reactor FRM-II (TU München, Garching, Germany), on the cold neutron time-of-flight spectrometer FOCUS (40) at the neutron spallation source SINQ (PSI, Villigen, Switzerland) and on the thermal neutron backscattering spectrometer IN13 (41) at the ILL high flux research reactor (ILL, Grenoble, France).

On TOFTOF, the incident wavelength was set to 5.1 Å and a chopper frequency of 12,000 rpm was chosen that corresponds to a scattering vector independent instrument resolution of ~100 μeV (full width at half-maximum, FWHM). Hb in solution was measured on TOFTOF between 280 K and 325 K. On FOCUS, the incident wavelength was set to 6 Å, which corresponds to only a moderately scattering vector dependent elastic energy resolution between 41 μeV (FWHM) at $q = 0.4$ Å^{-1} and 61 μeV (FWHM) at $q = 1.6$ Å^{-1}. Hydrated Hb powder was measured on FOCUS between 285 K and 322 K. The backscattering spectrometer IN13 is characterized by an energy resolution of 8 μeV (FWHM) and an incident wavelength of 2.23 Å. Hydrated Hb powder was measured between 20 K and 320 K on

IN13. All samples, including the vanadium slab and empty sample holder, were oriented at 135° with respect to the incident neutron beam direction.

The measured spectra were corrected for energy dependent detector efficiency, empty cell scattering, normalized to vanadium, transformed into energy transfer and scattering vector space, and corrected with a detailed balance factor. Data on IN13 were normalized to the recorded intensities at 20 K instead of vanadium. On IN13 elastic neutron scattering was measured between 0.2 $Å^{-1} \leq q \leq 5.0$ $Å^{-1}$. TOFTOF data were binned into 16 groups with 0.5 $Å^{-1} \leq q \leq 2.0$ $Å^{-1}$, FOCUS data were binned in 13 groups with 0.4 $Å^{-1} \leq q \leq 1.6$ $Å^{-1}$. QENS data reduction and analysis was done using the programs FRIDA for TOFTOF (42) and DAVE (43) for FOCUS data. IN13 data were reduced with ILL standard programs. Multiple scattering was neglected as the transmission of all samples was higher than 0.9.

The resolution function of the instruments was determined with vanadium measurements for TOFTOF and FOCUS. The instrumental energy resolutions of $\Delta E = 8$, 50, and 100 μeV correspond to observable timescales in the order of $\Delta t \sim 80$, 13, and 7 ps, respectively, using the relation $\Delta t = \hbar/\Delta E$.

Quasielastic neutron scattering analysis

An exhaustive description of quasielastic neutron scattering can be found in Bée (29). The application to protein dynamics has been reviewed by Gabel et al. (44) and Smith (22). QENS spectra in this study were well described with a theoretical scattering function $S_{\text{theo}}(q,\omega)$ that contains a delta-function for the fraction of hydrogen atoms that appear localized within the time-space window of the instrument and one Lorentzian $L(\omega,q)$ for the quasielastic signal,

$$S_{\text{theo}}(q,\omega) = A_0(q) \times \delta(\omega) + (1 - A_0(q)) \times L(q,\omega). \quad (1)$$

The elastic incoherent structure factor $A_0(q)$ (EISF) contains information about the geometry of motions. Mean-square displacements of fast vibrational motions $\langle u^2\rangle_{\text{vib}}$ (defined as the full amplitude of the motion (22)) were taken into account by a Debye-Waller factor $\exp(-\langle u^2\rangle_{\text{vib}} q^2/6)$ and were deduced from the scattering vector dependence of the summed intensities (19). The quasielastic component is a Lorentzian $L(q,\omega) = \frac{1}{\pi} \times \frac{\Gamma(q)}{\omega^2+\Gamma(q)^2}$, with half widths at half-maximum (HWHM) $\Gamma(q)$.

The scattering function $S(q,\omega)$ plus background was convoluted with the instrumental resolution function $S_{\text{res}}(q,\omega)$ and fitted to the measured data according to

$$S_{\text{meas}} = \left[\exp\left(-\langle u^2\rangle_{\text{vib}} q^2/6\right) \times S_{\text{theo}}(q,\omega) + B_0\right] \otimes S_{\text{res}}(q,\omega). \quad (2)$$

The fits were carried out over the energy transfer range from −1.5 meV to +1.5 meV for TOFTOF data and over the energy transfer range from −0.75 meV to +0.75 meV for FOCUS data.

Depending on the instrumental energy resolution and the used scattering vector range both internal protein dynamics and global translational diffusion of the macromolecules contribute to the measured signal in protein solution (13,15,17,18,45). Due to the high protein concentration of our solution sample, global protein diffusion is strongly suppressed and cannot be resolved with the energy resolution of 100 μeV of the spectrometer TOFTOF (19). In hydrated protein powders global macromolecular diffusion is absent. Therefore, it was possible to perform the experiment on FOCUS with a higher energy resolution of 50 μeV.

Elastic neutron scattering analysis

Elastic incoherent neutron scattering on IN13 was interpreted in terms of the Gaussian approximation. Mean-square displacements $\langle u^2\rangle$ were obtained from the scattering vector dependence of the elastic intensity $I(q)$ according to $\langle u^2\rangle = \frac{-6\times\Delta(\ln I(q))}{\Delta q^2}$, where we use the definition of $\langle u^2\rangle$ given by Smith that accounts for the full amplitude of motion (22). This approach is formally similar to the Guinier approximation in small angle scattering experiments (46). The analogy to small angle scattering has been discussed in (47,48). The obtained $\langle u^2\rangle$ describe the spatial extend of the atomic thermal motions and include both vibrational and diffusive dynamics. The approximation is strictly valid for $q^2 \to 0$ but holds up to $\langle u^2\rangle \times q^2 \sim 2$ (48). The calculations were carried out in the smallest accessible q^2-range of IN13 data between $0.04\ Å^{-2} \leq q^2 \leq 2.02\ Å^{-2}$ in which the Gaussian approximation is valid. Mean force constants $\langle k\rangle$ that describe the protein resilience were obtained from the slope of $\langle u^2\rangle$ versus temperature T according to $\langle k\rangle = 0.00276/(d\langle u^2\rangle/dT)$. Effective force constants $\langle k'\rangle$ that include anharmonic dynamics of proteins were calculated according to $\langle k'\rangle = 0.00276/(d\langle u^2\rangle/dT)$ in a quasi-harmonic approximation (31).

RESULTS

Quasielastic neutron scattering

Typical quasielastic neutron scattering spectra of hydrated Hb powder at 285 K measured on the spectrometer FOCUS and of Hb solution at 290 K measured on the instrument TOFTOF are shown in Fig. 1. The measured data could be described with an elastic peak for the hydrogen fraction that appears localized in the time-length scale given by the energy resolution and scattering vector range of the instrument, and one Lorentzian for diffusive internal protein dynamics.

Conclusions about protein internal motions can be drawn from the q dependences of the intensities and half-widths $\Gamma(q)$ of the elastic peaks and the Lorentzians, respectively. Information about the geometry of the motions is contained in the EISF $A_0(q)$, and about their correlation times in $\Gamma(q)$.

Hydrogen atoms that are covalently bound to amino acid side chains reflect the dynamical behavior of the bigger chemical units (21,23). The ''diffusion in a sphere'' model proposed by Volino and Dianoux (49) accounts well for the motions of amino acid side chains that perform diffusive jumps in a spherical volume restricted by neighboring amino acid side chains. The radius can then be deduced from

$$A_0(q) = p + (1-p) \times \left[\frac{3j_1(qa)}{qa}\right]^2, \quad (3)$$

where $j_1(qa)$ is the first-order spherical Bessel function of the first kind, a is the sphere radius, and $A_0(q)$ is the EISF (49). The populations of hydrogen atoms that appear as immobile and mobile within the instrumental energy resolution are represented by the fractions p and (1 - p), respectively (50).

A Gaussian distribution $f(a)$ of sphere radii a was used to describe measured EISF data of proteins to a high degree of accuracy (18). The Gaussian distribution is defined as $f(a) = \frac{2}{\sigma\sqrt{2\pi}}\exp(-a^2/2\sigma^2)$, with the standard deviation σ as free parameter. The mean value of the sphere radius is then given by $\widehat{a} = \sigma\sqrt{\frac{2}{\pi}}$. We recently measured Hb dynamics in whole red blood cells in vivo (15) and interpreted the obtained EISF with the model for diffusion in a sphere including a Gaussian distribution of sphere radii. For the

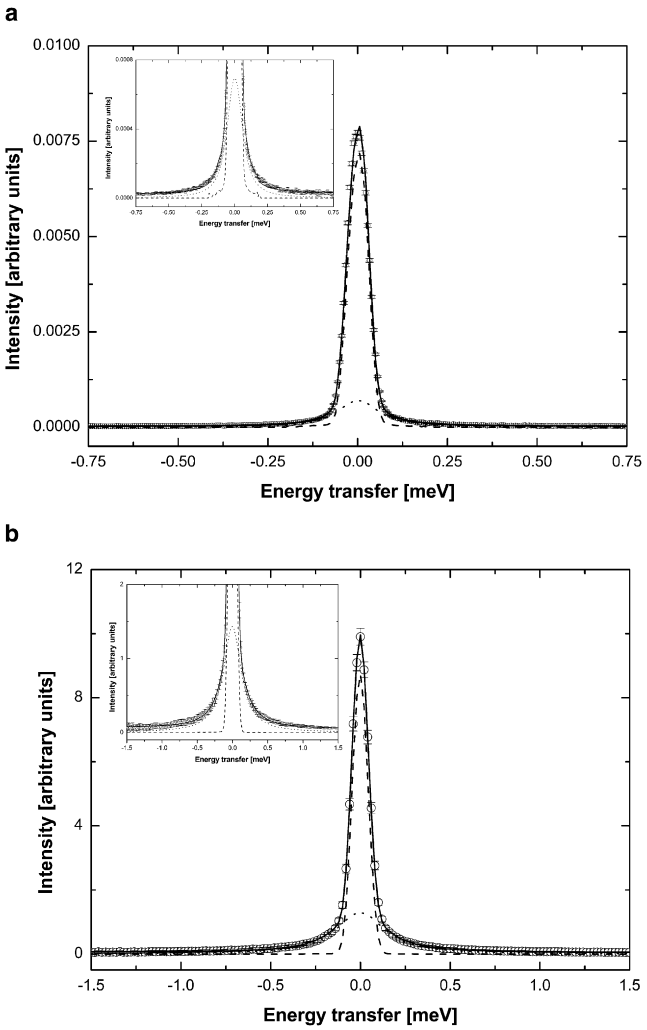

FIGURE 1 Quasielastic neutron spectra of (*a*) hydrated hemoglobin powder measured on FOCUS at the temperature 285 K at the scattering vector $q = 1.6$ Å^{-1}, and (*b*) hemoglobin in solution measured on TOFTOF at the temperature 290 K at the scattering vector $q = 1.8$ Å^{-1}. The circles show measured data and the solid line presents the fit (Eq. 2). The components correspond to the elastic fraction (*dashed line*) and the Lorentzian (*dotted line*). The insets in *a* and *b* show magnifications of the spectra.

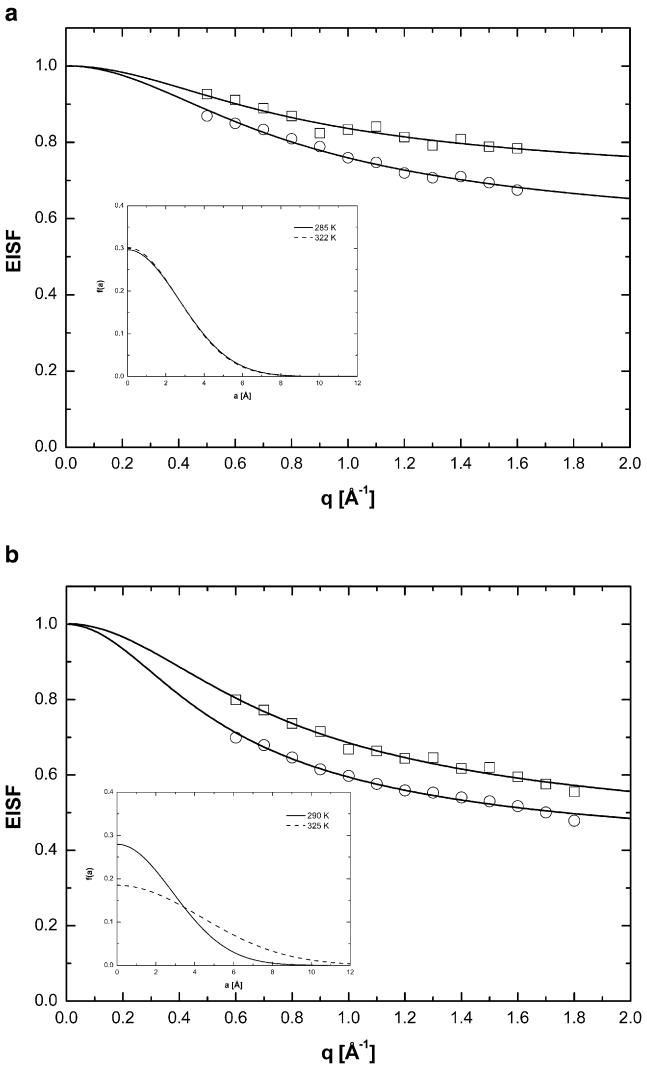

FIGURE 2 (*a*) EISF of hydrated hemoglobin powder at the temperatures 285 K (*squares*) and 322 K (*circles*) measured on FOCUS. (*b*) EISF of hemoglobin solution at the temperatures 290 K (*squares*) and 325 K (*circles*) measured on TOFTOF. The error bars are within the symbols. The solid lines present the fit (Eq. 3) with a Gaussian distribution $f(a)$ of radii. The insets in *a* and *b* show the distributions $f(a)$ at the indicated temperatures for hemoglobin powder and solution, respectively.

purpose of continuity and comparison with the previous study, we used this model to interpret the EISF of this work. Fits of the EISF were done over the scattering vector range of $q = 0.6$–1.8 Å^{-1} for TOFTOF and of $q = 0.5$–1.6 Å^{-1} for FOCUS. The EISF of Hb powder at the temperatures 285 K and 322 K and Hb solution at the temperatures of 290 K and 325 K are shown together with the fits of the model for diffusion in a sphere with a Gaussian distribution of radii in Fig. 2, *a* and *b*. The mean sphere radius $\hat{a}$ of the Gaussian distribution as a function of temperature is given in Fig. 3 for Hb powder and Hb solution. The mean radii of the hydrated powder sample remain constant in the investigated temperature range and have the average value of $\hat{a} = 2.06 \pm 0.02$ Å. The mean values $\hat{a}$ of the Hb solution sample show different behavior. Within the errors, they increase linearly with temperature between the values $\hat{a} = 2.27 \pm 0.06$ Å at 280 K and $\hat{a} = 2.58 \pm 0.09$ Å at 310 K. There is an inflection point at 310 K above which the mean sphere radii increase linearly with a significantly steeper slope up to 3.44 ± 0.09 Å at 325 K. The values of the immobile fraction were found to be constant with temperature for the concentrated Hb solution sample with $p = 0.38$ and to decrease linearly with increasing temperature for the Hb powder sample with $p = 0.67$ at 285 K and $p = 0.53$ at 322 K.

The half-widths at half-maximum Γ of the Lorentzian are shown in Fig. 4 as a function of the squared scattering vector q^2 at 285 K and 322 K for hydrated powder and at 290 K and

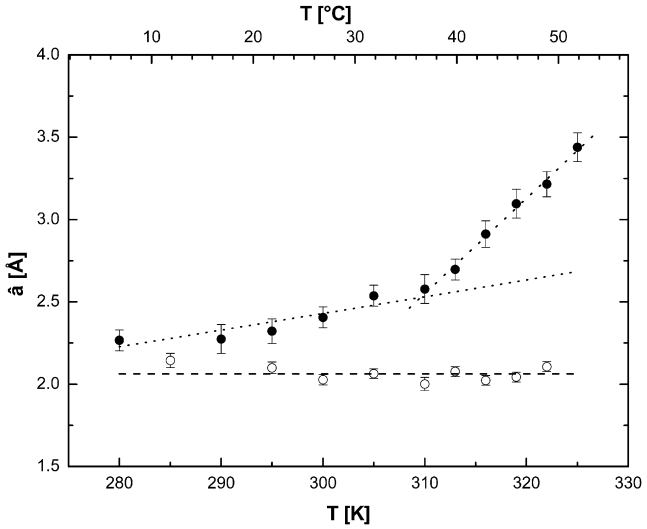

FIGURE 3 Mean value $\hat{a}$ of the Gaussian distribution as a function of temperature of hemoglobin in solution (*solid circles*) and hydrated hemoglobin powder (*open circles*). The dashed and dotted lines are linear fits and serve as a guide for the eye.

322 K for Hb solution. The measured half widths Γ of the Hb solution sample show clear signs for restricted jump-diffusion (51). The half widths Γ approach a constant value Γ_0 at small q^2 at 290 K. Small q^2-values correspond to larger real space distances and the effects of boundaries on the dynamics of amino acid side chains become visible. At the highest measured temperature of 322 K the plateau due to confinement would be visible only at very small q^2 values and is outside of the instrumental accessible scattering vector range as it was also found in protein solution (52). The limiting behavior of Γ at small q^2-values is approximately described by the Volino-Dianoux model for diffusion in confined geometry (49). The model assumes diffusion that

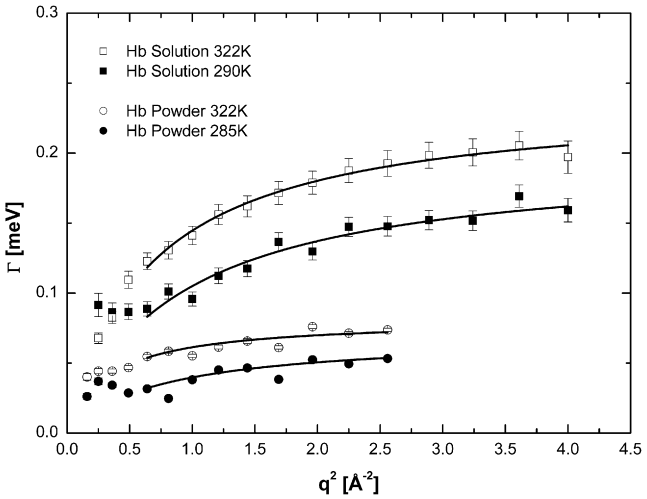

FIGURE 4 Half widths at half-maximum Γ of the Lorentzian as a function of scattering vector at different temperatures of hemoglobin in solution and as hydrated powder. The solid lines are fits according to a jump-diffusion model in the q^2-range from 0.64 $Å^{-2}$ to 4.0 $Å^{-2}$ and from 0.64 $Å^{-2}$ to 2.56 $Å^{-2}$.

is restricted to a sphere of radius a. It predicts constant half widths Γ_0 at q values smaller then $q < \pi/a$ (49). In the case of a distribution of sphere radii, the plateau ends at a smaller value q' than in the single sphere case as shown with molecular dynamics simulations (53). We extracted the scattering vector positions from the article of Dellerue et al. (53) and concluded that the value q' is ~1.7 times smaller for amino acid side chain dynamics than predicted by the Volino-Dianoux model for a single sphere of radius $\hat{a}$ that is the average value of the sphere distribution (53). In our work, at the temperature of 290 K the obtained mean sphere radius is $\hat{a} = 2.27$ Å and at 322 K the mean radius is $\hat{a} = 3.22$ Å. The constant value Γ_0 should therefore end at $q^2 = (\pi/1.7 \times \hat{a})^2 = 0.7 Å^{-2}$ at the temperature 290 K and at $q^2 = 0.3$ $Å^{-2}$ at the temperature 322 K. The q resolution of the experiment is not very precise but the constant value of Γ_0 at 290 K ends between $q^2 = 0.64$ $Å^{-2}$ and 0.81 $Å^{-2}$ that agrees well with the derived value from the model. The constant value at 322 K would therefore be visible only below $q^2 = 0.3$ $Å^{-2}$ that cannot be measured with the instrument. Additionally, this supports our assumption of a distribution of sphere radii to describe the measured EISF.

At large scattering vector values of the Hb solution sample, the elementary nature of the diffusive jumps of the amino acid side chains becomes evident. As these jumps are not infinitely small but occur over a finite length, the half-widths Γ approach asymptotically a plateau Γ_∞ at large q^2. The behavior of the half-widths can be described by a model of jump-diffusion according to $\Gamma = \frac{Dq^2}{1+Dq^2\tau}$, with the residence time before a jump τ and the jump-diffusion coefficient D (29). Fits were done with the jump-diffusion model in the q^2-range between 0.64 $Å^{-2}$ and 4.0 $Å^{-2}$. The obtained residence times follow the Arrhenius law $\tau(T) = \tau_0 \times e^{\frac{E_a}{k_B T}}$, and we extracted an activation energy of $E_a = 1.45 \pm 0.18$ kcal/mol.

The line-widths Γ of the Hb powder sample increase with q^2, which is a sign for diffusive motions. Similar behavior was already observed in hydrated lysozyme and myoglobin powders (17). The line-widths do not intercept zero at the smallest q^2-values, which is characteristic for diffusion in a confined space (29). For the purpose of comparison with the Hb solution, the half-widths of the Hb powder were also approximated with the jump-diffusion model as described above in the q^2-range of 0.64–2.56 $Å^{-2}$. The plateau Γ_∞ of the half-widths was obtained by extrapolation of the model to higher q^2-values. The residence times follow the Arrhenius law and we obtain an activation energy of $E_a = 1.70 \pm 0.12$ kcal/mol.

The half widths of the Hb solution are at all q^2-values and all temperatures larger than those of Hb powder. As correlation times and line widths are inversely correlated, the larger half widths of the Hb solution compared to the hydrated powder indicate that the rates of side chain diffusion get enhanced with increasing hydration.

In a recent work, we studied global macromolecular diffusion in red blood cells (protein concentration ~330 mg/mL) with neutron spectroscopy using an energy resolution of 50 μeV (FWHM) (15). Global protein diffusion in red blood cells is nearly to slow to be measured with an energy resolution of 50 μeV. Global macromolecular diffusion is even stronger reduced at the high concentration of 570 mg/mL and appears nearly static at the instrumental energy resolution of 100 μeV (FWHM) and the accessible scattering vector range. This was already shown by Jasnin et al. (14) and Tehei et al. (19). Gabel studied the contribution of global macromolecular diffusion to mean-square displacements $\langle u^2 \rangle$ determined with elastic neutron scattering (47). The author concluded that global macromolecular diffusion results in 7% larger $\langle u^2 \rangle$ when using an instrumental energy resolution of 100 μeV and a scattering vector range of 1–4Å^{-2}. As a check, we tried to fit the data for Hb solution with two Lorentzians: a narrow one for global macromolecular diffusion and a broad one for internal protein dynamics. The obtained HWHM of the broad component are a factor three larger at all temperatures and all scattering vector values then the HWHM shown in Fig. 4. The HWHM are then too large and do not agree with values reported in literature (14,15,19,52,54). The HWHM of the narrow component show linear behavior as a function of q^2. However, the obtained diffusion coefficients are a factor two to three too large as compared to expected values (55).

Elastic neutron scattering

Mean-square displacements $\langle u^2 \rangle$ of hydrated Hb powder measured on IN13 were calculated from the data in the q^2-range up to $q^2 = 2.02$ Å^{-2} and are given in Fig. 5. The

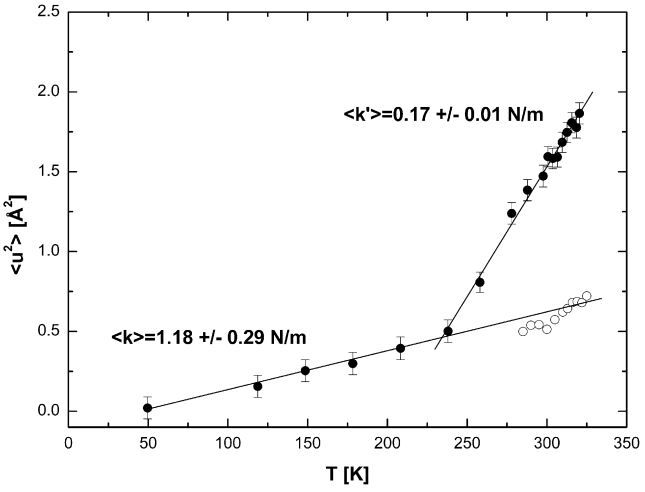

FIGURE 5 Mean-square displacements $\langle u^2 \rangle$ of hydrated hemoglobin powder measured on IN13 (*solid circles*) and mean-square displacements of fast vibrational motions $\langle u^2 \rangle_{vib}$ (using Eqs. 1 and 2) measured on FOCUS (*open circles*). The error bars of $\langle u^2 \rangle_{vib}$ are within the symbols. The straight lines are linear fits to $\langle u^2 \rangle$ measured on IN13 below and above the dynamical transition temperature. The energy resolution of IN13 is 8 μeV.

$\langle u^2 \rangle$ include both vibrational and diffusive motions of protein dynamics and show the well known dynamical transition at ~240 K (8,9,56). Values of the force constants of $\langle k \rangle = 1.18 \pm 0.29$ N/m for the low temperature range below 240 K and $\langle k' \rangle = 0.17 \pm 0.01$ N/m for the high temperature range above 240 K were obtained. QENS experiments allow the separation of vibrational and diffusive dynamics. Mean-square displacements of fast vibrational motions $\langle u^2 \rangle_{vib}$ of the Hb powder sample measured with QENS on FOCUS are presented in Fig. 5. The $\langle u^2 \rangle_{vib}$ agree with good accuracy with expected values obtained from linear extrapolation of the low temperature vibrational values $\langle u^2 \rangle$ measured on IN13.

DISCUSSION

It has been reported previously in the literature that protein flexibility is linked to protein structure. Gaspar et al. (45) investigated the dynamics of proteins that consist purely of β-sheet, α-helix, both α- and β-structure elements and unstructured proteins. The authors reported that β-sheet proteins are the least flexible, followed by α-helical proteins. Proteins that consist of both α- and β-structure elements are more flexible than pure α-helical proteins and unstructured proteins were found to be the most flexible ones (45). Additionally, it has been shown that the unfolded state of lysozyme is more flexible and less resilient than the folded state (57). Consistently with these results, neutron scattering measurements of whole bacteria in vivo showed that average protein flexibility is increased and macromolecular resilience is reduced in heat denatured bacteria cells as compared to native cells (16). Furthermore, protein flexibility, resilience and internal diffusion rates have been found to be closely linked to the degree of hydration. Neutron scattering combined with hydrogen/ deuterium labeling of specific amino acids allowed the determination of average protein dynamics and active core fluctuations of bacteriorhodopsin as a function of hydration. Increasing the level of hydration from dry powder to a complete hydration layer coverage of bacteriorhodopsin permitted the onset of anharmonic motions above the dynamical transition temperature of ~180–240 K at a certain threshold hydration; a further increase of hydration led to a decrease of protein resilience (11,12,24,58). Neutron scattering measurements of dry and hydrated protein powders, as well as of protein solution showed that the rates and amplitudes of amino acid side chains diffusion on the protein surface are enhanced with higher hydration (17,59). Further work on protein dynamics under physiological conditions in *Escherichia coli* showed that hydrated powders do not accurately represent the dynamical behavior of macromolecules in whole cells. The higher amount of water in cells, as compared to fully hydrated protein powders, increases internal molecular flexibility and diffusive motion rates in the picosecond time-range (14). Colombo et al. (60) studied hydration changes between the fully deoxygenated tense (T) form and the fully oxygenated relaxed (R) form of Hb. The

authors reported that ~60 extra water molecules are bound in the R state compared to the T state. The additional water molecules were found to be thermodynamically important for functional regulation of Hb. Caronna et al. (61) studied the dynamics of Hb in the T and R state with high resolution neutron spectroscopy. In the nanosecond timescale the structure of Hb in the R state is slightly more flexible and less rigid than in the T state, which is in agreement with the assumption that the ~60 extra water molecules in the R state contribute to a larger flexibility of the protein. However, it was also reported that faster protein motions in the order of ~100 ps are not influenced by the quaternary structure of Hb (61). Consequently, the dynamics of Hb in different quaternary states are expected to be similar if not identical in the order of some picoseconds, which is the timescale of our study.

We verified with EINS that the well know dynamical transition at ~240 K occurs at the chosen hydration of the Hb powder sample. At low temperatures only solid-like vibrational motions are detected; at temperatures above the dynamic transition temperature protein specific quasi-diffusive motions are activated and contribute to the measured $\langle u^2 \rangle$ (56). From QENS experiments vibrational and diffusive motions can be separated. As expected, the obtained vibrational motions $\langle u^2 \rangle_{\mathrm{vib}}$ are in good agreement with linear extrapolation of low temperature $\langle u^2 \rangle$ obtained from the EINS measurement. This supports the concept of quasi-diffusive motions in proteins being activated at the dynamic transition temperature that cause the pronounced increase of $\langle u^2 \rangle$ at higher temperatures (28,56).

Our experiments showed that increasing hydration of Hb has a strong influence on the rates of diffusive motions. The residence times of amino acid side chain jump-diffusion in Hb solution lie between $\tau = 4.0 \pm 0.2$ ps at 280 K and 2.8 ± 0.1 ps at 322 K, whereas we obtain significantly higher residence times between $\tau = 10.3 \pm 0.3$ ps at 285 K and $\tau = 7.6 \pm 0.4$ ps at 325 K for hydrated Hb powder. The obtained activation energy E_a of the residence times raises from 1.45 ± 0.18 kcal/mol for Hb solution to 1.70 ± 0.12 kcal/mol for hydrated Hb powder. We conclude that an increase of hydration from a single layer to nearly three layers enhances the rates of diffusive motions. The supplementary amount of water decreases the activation energy barriers between diffusive jumps and thus facilitates protein dynamics, as shown with QENS. In the Fraunfelder et al. (28) study, proteins exist in many slightly different conformational substates that are separated by activation energy barriers. The sampling of the conformational substates contributes to the entropic stabilization of proteins. Lower activation energy barriers allow an increased sampling rate of the conformational substates. The other term that determines protein stability is the enthalpic contribution that is determined by the macromolecular force field (31).

Artmann et al. (2) reported a transition temperature of human Hb at body temperature that was interpreted as Hb partial unfolding and acts as a precursor for protein aggregation. Partial unfolding of human Hb was independent of the oxygenation state and also occurred for sickle cell Hb in the oxygenated state (5). Partial unfolding of human Hb was fully reversible at least up to 39°C (5). Human Hb aggregation and thermal stability of the Hb tetramer was studied with small angle neutron scattering (unpublished data). Hb aggregation was found to be reversible up to 40°C, the Hb tetramer was found to be stable at least up to 44°C. Dissociation into dimers would lead to a higher colloidal osmotic pressure rather than a lower one as observed previously (1). Further evidence for perturbations of Hb secondary structure at a specific transition temperature came from CD experiments (6,7). These studies of Digel et al. (6) and Zerlin et al. (7) established the fact that the transition temperature of Hb from a big variety of different animals is directly linked to body temperature of the species. Sequence alignments of Hb of different species were carried out to identify an eventual region for the structural perturbation (7). Hb tertiary structure is highly conserved in general. However, it was found that the amino acid sequences of the first two helices of the α- and β-subunits of Hb were of low similarity (~40–50% similarity) and are solvent exposed. The other parts have significantly higher similarity (~70–80% similarity), and especially the inner parts of the protein that are in close contact to the heme groups are highly conserved (up to 100% similarity). It was suggested that these solvent-exposed amino acid residues might be responsible for the onset of Hb partial unfolding and protein aggregation (7).

A study of Engler et al. (62) classified hydrogen atoms in myoglobin in three dynamic groups: methyl group, long side chain, and backbone hydrogen atoms. The authors concluded that above the dynamical transition mean-square displacements measured by neutron scattering are dominated by the side chains on a timescale faster than 100 ps (62). Therefore, in this study, we used the model of diffusion in a sphere (49) that is best suited to describe amino acid side chain diffusion. Amino acid side chain dynamics within proteins were found to be characterized by a distribution of flexibility. Side chains in the protein interior are more rigid, whereas they possess a higher degree of flexibility toward the outside of the protein (53). The term flexibility corresponds in this sense to the restricted volume in which the amino acid side chains can move. Therefore, we used an extended version of the diffusion in a sphere model, which takes into account of a distribution of sphere radii (15,17,18). We do not claim that the model by Volino and Dianoux (49) that implies motions in a sphere with impermeable surface is the most appropriate one to describe the atomic nature of protein dynamics. However, it is able to describe the measured EISF with high accuracy. As we are mostly interested in the temperature dependence of protein flexibility, it is a valid approach to use this model for the purpose of comparison.

Alternative models for the interpretation of protein dynamics are the double well model proposed by Doster

et al. (8), the quasi-harmonic approximation by Bicout and Zaccai (30), the Brownian oscillator by Knapp et al. (63) or the fractional Brownian dynamics model by Kneller (64). Especially the models proposed by Knapp et al. (63) and Kneller (64) might be relevant for the interpretation of QENS data. Molecular dynamics simulations yield detailed atomistic information about protein dynamics in the picosecond and nanosecond timescale. The simulations allow a direct comparison with neutron experiments and facilitate the interpretation of the measured QENS spectra. It would be of high interest to carry out molecular dynamics simulations of hydrated Hb and to study the temperature behavior of Hb dynamics around body temperature.

In recent studies of Hb dynamics in red blood cells, the break at 310 K in the sphere radii was interpreted as partial unfolding of Hb at human body temperature (15). The same interpretation is valid for the results of Hb in concentrated solution. In this sense, the partially unfolded state of Hb solution at temperatures above 310 K has got higher flexibility than the low temperature state, as its distribution is shifted to larger volumes. It is not known, if protein aggregation influences protein dynamics. However, protein aggregation would rather lead to a reduction and not to an increase in flexibility, as observed in our study. Therefore, in the time-space window of the neutron spectrometer we conclude that protein aggregation has a minor influence on protein flexibility. The fact that partial unfolding and the consequent changes of dynamics do not occur in hydrated powder implies a crucial role of hydration in this process. It was previously suggested that solvent accessible amino acid side chains might be responsible for Hb partial unfolding (6,7). The observed changes in the dynamics of amino acid side chains at body temperature might be responsible for an increase in surface hydrophobicity that promotes protein association and aggregation (15). The trigger for Hb aggregation would be body temperature. The experimental facts presented in this work justify this view. Diffusive motion rates of side chains are strongly suppressed in hydrated Hb powder as compared to Hb in concentrated solution. We concluded previously that protein dynamics and changes in the complex macromolecular force field might be responsible for structural rearrangements and pronounced protein aggregation above body temperature (15). The molecular properties of Hb therefore could determine in this sense the macroscopic properties of whole red blood cells (2). We identified a fast process in the order of some picoseconds that is responsible for the change in geometry of protein dynamics at body temperature. A sufficient level of hydration beyond one surface layer is crucial for the activation of this fast process.

We thank Prof. Dr. Judith Peters and Dr. Francesca Natali for assistance on the instrument IN13, and Dr. Marion Jasnin for fruitful discussion and critical reading of the manuscript. This study is based on experiments carried out at FRM-II, TU München, Garching, Germany, at SINQ, PSI, Villigen, Switzerland, and at ILL, Grenoble, France.

This work was supported by the European Commission under the 6th Framework Programme through the Key Action: Strengthening the European Research Area, Research Infrastructures (RII3-CT-2003-505925), the Institut Laue-Langevin (M.T.), and the AINSE (M.T.).

REFERENCES

1. Artmann, G. M., K. F. Zerlin, and I. Digel. 2008. Hemoglobin senses body temperature. *In* Bioengineering in Cell and Tissue Research. G. M. Artmann and S. Chien, editors. Springer Verlag, Berlin, Heidelberg, pp. 415–447.
2. Artmann, G. M., C. Kelemen, D. Porst, G. Büldt, and S. Chien. 1998. Temperature transitions of protein properties in human red blood cells. *Biophys. J.* 75:3179–3183.
3. Krueger, S., and R. Nossal. 1988. SANS studies of interacting hemoglobin in intact erythrocytes. *Biophys. J.* 53:97–105.
4. Kelemen, C., S. Chien, and G. M. Artmann. 2001. Temperature transition of human hemoglobin at body temperature: effects of calcium. *Biophys. J.* 80:2622–2630.
5. Artmann, G. M., L. Burns, J. M. Canaves, A. Temiz-Artmann, G. W. Schmid-Schonbein, et al. 2004. Circular dichroism spectra of human hemoglobin reveal a reversible structural transition at body temperature. *Eur. Biophys. J.* 33:490–496.
6. Digel, I., C. Maggakis-Kelemen, K. F. Zerlin, P. Linder, N. Kasischke, et al. 2006. Body temperature-related structural transitions of monotremal and human hemoglobin. *Biophys. J.* 91:3014–3021.
7. Zerlin, K. F., N. Kasischke, I. Digel, C. Maggakis-Kelemen, A. Temiz Artmann, et al. 2007. Structural transition temperature of hemoglobins correlates with species' body temperature. *Eur. Biophys. J.* 37:1–10.
8. Doster, W., S. Cusack, and W. Petry. 1989. Dynamical transition of myoglobin revealed by inelastic neutron scattering. *Nature*. 337:754–756.
9. Ferrand, M., A. J. Dianoux, W. Petry, and G. Zaccai. 1993. Thermal motions and function of bacteriorhodopsin in purple membranes—effects of temperature and hydration studied by neutron-scattering. *Proc. Natl. Acad. Sci. USA*. 90:9668–9672.
10. Cornicchi, E., M. Marconi, G. Onori, and A. Paciaroni. 2006. Controlling the protein dynamical transition with sugar-based bioprotectant matrices: a neutron scattering study. *Biophys. J.* 91:289–297.
11. Paciaroni, A., S. Cinelli, and G. Onori. 2002. Effect of the environment on the protein dynamical transition: a neutron scattering study. *Biophys. J.* 83:1157–1164.
12. Paciaroni, A., E. Cornicchi, A. De Francesco, M. Marconi, and G. Onori. 2006. Conditioning action of the environment on the protein dynamics studied through elastic neutron scattering. *Eur. Biophys. J.* 35:591–599.
13. Doster, W., and S. Longeville. 2007. Microscopic diffusion and hydrodynamic interactions of hemoglobin in red blood cells. *Biophys. J.* 93:1360–1368.
14. Jasnin, M., M. Moulin, M. Haertlein, G. Zaccai, and M. Tehei. 2008. In vivo measurement of internal and global macromolecular motions in E. coli. *Biophys. J.* 95:857–864.
15. Stadler, A. M., I. Digel, G. M. Artmann, J. P. Embs, G. Zaccai, et al. 2008. Hemoglobin dynamics in red blood cells: correlation to body temperature. *Biophys. J.* 95:5449–5461.
16. Tehei, M., B. Franzetti, D. Madern, M. Ginzburg, B. Z. Ginzburg, et al. 2004. Adaptation to extreme environments: macromolecular dynamics in bacteria compared in vivo by neutron scattering. *EMBO Rep.* 5:66–70.
17. Perez, J., J. M. Zanotti, and D. Durand. 1999. Evolution of the internal dynamics of two globular proteins from dry powder to solution. *Biophys. J.* 77:454–469.
18. Russo, D., J. Perez, J. M. Zanotti, M. Desmadril, and D. Durand. 2002. Dynamic transition associated with the thermal denaturation of a small beta protein. *Biophys. J.* 83:2792–2800.
19. Tehei, M., J. C. Smith, C. Monk, J. Ollivier, M. Oettl, et al. 2006. Dynamics of immobilized and native Escherichia coli dihydrofolate

reductase by quasielastic neutron scattering. *Biophys. J.* 90:1090–1097.

20. Sears, V. F. 1992. Neutron scattering lengths and cross sections. *Neutron News.* 3:26–37.
21. Reat, V., H. Patzelt, M. Ferrand, C. Pfister, D. Oesterhelt, et al. 1998. Dynamics of different functional parts of bacteriorhodopsin: H-2H labeling and neutron scattering. *Proc. Natl. Acad. Sci. USA.* 95:4970–4975.
22. Smith, J. C. 1991. Protein dynamics—comparison of simulations with inelastic neutron-scattering experiments. *Q. Rev. Biophys.* 24:227–291.
23. Wood, K., S. Grudinin, B. Kessler, M. Weik, M. Johnson, et al. 2008. Dynamical heterogeneity of specific amino acids in bacteriorhodopsin. *J. Mol. Biol.* 380:581–591.
24. Lehnert, U., V. Reat, M. Weik, G. Zaccai, and C. Pfister. 1998. Thermal motions in bacteriorhodopsin at different hydration levels studied by neutron scattering: correlation with kinetics and light-induced conformational changes. *Biophys. J.* 75:1945–1952.
25. Roh, J. H., J. E. Curtis, S. Azzam, V. N. Novikov, I. Peral, et al. 2006. Influence of hydration on the dynamics of lysozyme. *Biophys. J.* 91:2573–2588.
26. Roh, J. H., V. N. Novikov, R. B. Gregory, J. E. Curtis, Z. Chowdhuri, et al. 2005. Onsets of anharmonicity in protein dynamics. *Phys. Rev. Lett.* 95:038101.
27. Wood, K., M. Plazanet, F. Gabel, B. Kessler, D. Oesterhelt, et al. 2007. Coupling of protein and hydration-water dynamics in biological membranes. *Proc. Natl. Acad. Sci. USA.* 104:18049–18054.
28. Fraunfelder, H., S. G. Sligar, and P. G. Wolynes. 1991. The energy landscapes and motions of proteins. *Science.* 254:1598–1603.
29. Bee, M. 1988. Quasielastic Neutron Scattering. Principles and Applications in Solid State Chemistry, Biology and Materials Science.. Adam Hilger, Bristol and Philadelphia.
30. Bicout, D. J., and G. Zaccai. 2001. Protein flexibility from the dynamical transition: a force constant analysis. *Biophys. J.* 80:1115–1123.
31. Zaccai, G. 2000. How soft is a protein? A protein dynamics force constant measured by neutron scattering. *Science.* 288:1604–1607.
32. Tehei, M., D. Madern, C. Pfister, and G. Zaccai. 2001. Fast dynamics of halophilic malate dehydrogenase and BSA measured by neutron scattering under various solvent conditions influencing protein stability. *Proc. Natl. Acad. Sci. USA.* 98:14356–14361.
33. Tehei, M., and G. Zaccai. 2007. Adaptation to high temperatures through macromolecular dynamics by neutron scattering. *FEBS J.* 274:4034–4043.
34. Ball, P. 2008. Water as an Active Constituent in Cell Biology. *Chem. Rev.* 108:74–108.
35. Rupley, J. A., and G. Careri. 1991. Protein hydration and function. *Adv. Protein Chem.* 41:37–172.
36. Alberts, B., A. J. Lewis, M. Raff, K. Roberts, and P. Walter. 2002. Molecular Biology of the Cell. Garland Science, New York.
37. Gabel, F., M. Weik, B. P. Doctor, A. Saxena, D. Fournier, et al. 2004. The influence of solvent composition on global dynamics of human butyrylcholinesterase powders: a neutron-scattering study. *Biophys. J.* 86:3152–3165.
38. Perutz, M. F., A. R. Fersht, S. R. Simon, and G. C. Roberts. 1974. Influence of globin structure on the state of the heme. II. Allosteric transitions in methemoglobin. *Biochemistry.* 13:2174–2186.
39. Unruh, T., J. Neuhaus, and W. Petry. 2007. The high-resolution time-of-flight spectrometer TOFTOF. *Nucl. Instrum. Methods Phys. Res. A.* 580:1414–1422.
40. Janssen, S., J. Mesot, L. Holitzner, A. Furrer, and R. Hempelmann. 1997. FOCUS: a hybrid TOF-spectrometer at SINQ. *Physica B (Amsterdam).* 234:1174–1176.
41. Natali, F., J. Peters, D. Russo, S. Barbieri, C. Chiapponi, et al. 2008. IN13 backscattering spectrometer at ILL: looking for motions in biological macromolecules and organisms. *Neutron News.* 19:14–18.
42. Wuttke, J. 2006. FRIDA (fast reliable inelastic data analysis). http://sourceforge.net/projects/frida.
43. DAVE Data Analysis and Visualization Environment.http://www.ncnr.nist.gov/dave2008.
44. Gabel, F., D. Bicout, U. Lehnert, M. Tehei, M. Weik, et al. 2002. Protein dynamics studied by neutron scattering. *Q. Rev. Biophys.* 35:327–367.
45. Gaspar, A. M., M. S. Appavou, S. Busch, T. Unruh, and W. Doster. 2008. Dynamics of well-folded and natively disordered proteins in solution: a time-of-flight neutron scattering study. *Eur. Biophys. J.* 37:573–582.
46. Guinier, A., and G. Fournet. 1955. Small Angle Scattering of X-Rays. Wiley, New York.
47. Gabel, F. 2005. Protein dynamics in solution and powder measured by incoherent elastic neutron scattering: the influence of Q-range and energy resolution. *Eur. Biophys. J.* 34:1–12.
48. Réat, V., G. Zaccai, M. Ferrand, and C. Pfister. 1997. Functional dynamics in purple membranes. *In* Biological Macromolecular Dynamics. S. Cusack, H. Buttner, M. Ferrand, P. Langan, and P. Timmins, editors. Adenine Press, New York. 117–122.
49. Volino, F., and A. J. Dianoux. 1980. Neutron incoherent-scattering law for diffusion in a potential of spherical-symmetry—general formalism and application to diffusion inside a sphere. *Mol. Phys.* 41:271–279.
50. Bellissent-Funel, M. C., J. Teixeira, K. F. Bradley, and S. H. Chen. 1992. Dynamics of hydration water in protein. *J. Phys. I. France.* 2:995–1001.
51. Hall, P. L., and D. K. Ross. 1981. Incoherent neutron scattering functions for random jump diffusion in bounded and infinite media. *Mol. Phys.* 42:673–682.
52. Bu, Z., D. A. Neumann, S. H. Lee, C. M. Brown, D. M. Engelmann, et al. 2000. A view of dynamics changes in the molten globule-native folding step by quasielastic neutron scattering. *J. Mol. Biol.* 301:525–536.
53. Dellerue, S., A. J. Petrescu, J. C. Smith, and M. C. Bellissent-Funel. 2001. Radially softening diffusive motions in a globular protein. *Biophys. J.* 81:1666–1676.
54. Bu, Z., J. Cook, and D. J. E. Callaway. 2001. Dynamic regimes and correlated structural dynamics in native and denatured alpha-lactalbumin. *J. Mol. Biol.* 312:865–873.
55. Tokuyama, M., and I. Oppenheim. 1994. Dynamics of hard-sphere suspensions. Phys. Rev. E Stat. Phys. Plasmas Fluids Relat. Interdiscip. *Topics.* 50:R16–R19.
56. Parak, F., E. W. Knapp, and D. Kucheida. 1982. Protein dynamics. Mossbauer spectroscopy on deoxymyoglobin crystals. *J. Mol. Biol.* 161:177–194.
57. De Francesco, A., M. Marconi, S. Cinelli, G. Onori, and A. Paciaroni. 2004. Picosecond internal dynamics of lysozyme as affected by thermal unfolding in nonaqueous environment. *Biophys. J.* 86:480–487.
58. Wood, K., U. Lehnert, B. Kessler, G. Zaccai, and D. Oesterhelt. 2008. Hydration dependence of active core fluctuations in bacteriorhodopsin. *Biophys. J.* 95:194–202.
59. Marconi, M., E. Cornicchi, G. Onori, and A. Paciaroni. 2008. Comparative study of protein dynamics in hydrated powders and in solution: A neutron scattering investigation. *Chem. Phys.* 345:224–229.
60. Colombo, M. F., D. C. Rau, and V. A. Parsegian. 1992. Protein solvation in allosteric regulation: a water effect on hemoglobin. *Science.* 256:655–659.
61. Caronna, C., F. Natali, and A. Cupane. 2005. Incoherent elastic and quasi-elastic neutron scattering investigation of hemoglobin dynamics. *Biophys. Chem.* 116:219–225.
62. Engler, N., A. Ostermann, N. Niimura, and F. Parak. 2003. Hydrogen atoms in proteins: positions and dynamics. *Proc. Natl. Acad. Sci. USA.* 100:10243–10248.
63. Knapp, E. W., S. F. Fischer, and F. Parak. 1982. Protein dynamics from Mossbauer spectra. The temperature dependence. *J. Phys. Chem.* 86:5042–5047.
64. Kneller, G. R. 2005. Quasielastic neutron scattering and relaxation processes in proteins: analytical and simulation-based models. *Phys. Chem. Chem. Phys.* 7:2641–2655.